

# Competition between group interactions and nonlinearity in voter dynamics on hypergraphs

Jihye Kim,<sup>1,2</sup> Deok-Sun Lee,<sup>2,3,\*</sup> Byungjoon Min,<sup>4,†</sup> Mason A. Porter,<sup>5,6,7,‡</sup> Maxi San Miguel,<sup>8,§</sup> and K.-I. Goh<sup>1,5,¶</sup>

<sup>1</sup>Department of Physics, Korea University, Seoul 02841, Korea

<sup>2</sup>School of Computational Sciences, Korea Institute for Advanced Study, Seoul 02455, Korea

<sup>3</sup>Center for AI and Natural Sciences, Korea Institute for Advanced Study, Seoul 02455, Korea

<sup>4</sup>Department of Physics, Chungbuk National University, Cheongju, Chungbuk 28644, Korea

<sup>5</sup>Department of Mathematics, University of California, Los Angeles, Los Angeles, CA 90095, USA

<sup>6</sup>Department of Sociology, University of California, Los Angeles, Los Angeles, CA 90095, USA

<sup>7</sup>Santa Fe Institute, Santa Fe, NM 87501, USA

<sup>8</sup>Instituto de Física Interdisciplinar y Sistemas Complejos, IFISC (CSIC-UIB),

Campus Universitat Illes Balears, E-07122 Palma de Mallorca, Spain

(Dated: July 17, 2024)

Social dynamics are often driven by both pairwise (i.e., dyadic) relationships and higher-order (i.e., polyadic) group relationships, which one can describe using hypergraphs. To gain insight into the impact of polyadic relationships on dynamical processes on networks, we formulate and study a polyadic voter process, which we call the *group-driven voter model* (GVM), in which we incorporate the effect of group interactions by nonlinear interactions that are subject to a group (i.e., hyperedge) constraint. By examining the competition between nonlinearity and group sizes, we show that the GVM achieves consensus faster than standard voter-model dynamics, with an optimum minimizing exit time  $\tau$ . We substantiate this finding by using mean-field theory on annealed uniform hypergraphs with  $N$  nodes, for which  $\tau$  scales as  $\mathcal{A} \ln N$ , where the prefactor  $\mathcal{A}$  depends both on the nonlinearity and on group-constraint factors. Our results reveal how competition between group interactions and nonlinearity shapes GVM dynamics. We thereby highlight the importance of such competing effects in complex systems with polyadic interactions.

**Introduction**—Individuals in society interact both in pairs and through various types of social groups (including families, clubs, and work colleagues) [1, 2]. Group (i.e., “polyadic”) interactions often are not merely structural units of a network; they also constitute functional units that drive dynamics through nonlinear effects [3, 4]. Consequently, the traditional network framework — which employs graphs and thus entails that group interactions are represented as collections of pairwise (i.e., dyadic) interactions [5] — has a fundamental limitation. To explicitly capture group interactions, one can employ “higher-order” (i.e., polyadic) network frameworks [5–8]. There has been much recent work on dynamical processes on polyadic networks [9–20] on a variety of systems, including opinion dynamics [21–26]. However, researchers still do not have a generic understanding of the impact of group interactions on dynamical processes.

To gain insights into the impact of group interactions on opinion dynamics, we formulate and analyze a polyadic voter model. Voter models (VMs) [27] are both among the simplest models of social dynamics [28] and among the best-understood theoretical models of collective behavior of complex systems [29, 30]. One can interpret the update rules of a VM [31] in terms of choosing between binary choices, which we denote by  $\sigma = 0$  and  $\sigma = 1$ . At each time step, a uniformly random node adopts the opinion of a uniformly random neighbor. (Henceforth, we use the term “random” as a shorthand description for uniformly at random.) VMs have been studied for more than half of a century [32], and VMs have been studied actively on traditional networks (i.e., graphs) for more than two decades [33–39]. VMs have also been extended in a variety of ways [40]. However, few of these studies account explicitly for group interactions [25, 26].

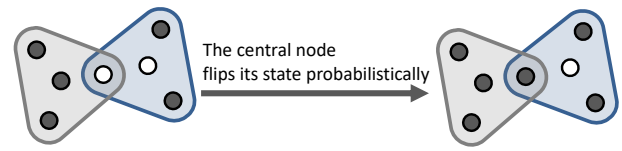


FIG. 1. Schematic illustration of our group-driven voter model (GVM) on a 4-uniform hypergraph. The central node flips ( $\circ \rightarrow \bullet$ ) with a probability that depends on the GVM update rule. For example, for the simplicial GVM its flip probability is  $1/2$ , as the central node has to pick the gray hyperedge to flip its state. For the GVM with nonlinearity strength  $q = 2$  and duplicate choices allowed, the central node’s flip probability is instead  $13/18$ . For the blue hyperedge, it has to select twice among its two black neighbors out of its three total neighbors.

The framework of polyadic networks can help fill this gap by providing explicit structural models, such as hypergraphs and simplicial complexes [5], to deal with group interactions. To incorporate group interactions into opinion dynamics, we use hypergraphs and generalize VM dynamics. To initiate our generalization, we first reformulate a traditional dyadic VM update rule by focusing on the role of edges. At each time step, a random node  $i$  chooses one of its edges (i.e., links) at random, and it flips its state  $\sigma_i$  to the state  $\sigma_j$  of the adjacent node  $j$  that is attached to the chosen edge if the states are different. In a dyadic network, each of these edges of a node  $i$  is attached to exactly 1 other node.

**Group-driven voter model**—In a hypergraph, a node  $i$  can be adjacent to more than one other node via a hyperedge. Each node in a hyperedge with cardinality (i.e., “size”)  $s$  is adjacent to  $s - 1$  nodes. This multiplicity leads to a broad

spectrum of possibilities for dynamical processes on hypergraphs. To investigate these possibilities, we study a *group-driven voter model* (GVM). At each time step, a random node  $i$  considers adopting an opinion from one of its incident hyperedge  $h$ , which we choose randomly. During the adoption process, node  $i$  makes  $q$  observations of states (i.e., opinions) of random nodes of hyperedge  $h$ . One can either allow [41] or disallow [42] duplicate choices of the same neighbor. If the  $q$  observed node states  $\{\sigma_{j_1}, \sigma_{j_2}, \dots, \sigma_{j_q} \mid j_p \in h \setminus \{i\}\}$  are unanimously different from its own state  $\sigma_i$ , then node  $i$  flips its state (see Fig. 1) to match the observed state.

Our model has two independent parameters:  $q$  and  $s$ . The parameter  $q$  accounts for nonlinear interactions [43], which are absent in the standard VMs but have been considered in nonlinear variants of voter models [41, 44–47]. The parameter  $s$  accounts for the effect of polyadic interactions. The GVM incorporates social reinforcement [42, 48–50] via group interactions [12, 51], suggesting an explicit group-based origin of nonlinearity, which has been introduced in an ad hoc way in various dyadic variants of VMs [52], including vacillating voter model [44], a  $q$ -voter model [41], a confident voter model [45], and nonlinear voter model [47].

The GVM has a variety of interesting special cases for particular values of  $q$  and  $s$ . When  $q = s - 1$  and duplicate choices are disallowed, the GVM captures the strongest group interactions, as it requires that all of the  $s - 1$  nodes' states of a selected hyperedge are unanimously different from node  $i$ 's state for node  $i$  to flip its state. This amounts to a “simplicial rule” [10], so we refer to this special case as a “simplicial GVM”. When  $q = 1$  for all values of  $s$ , the GVM essentially reduces to a standard dyadic VM; it loses the effects of polyadic interactions. Additionally, the GVM on dyadic networks ( $s = 2$ ) reduces to the standard VM for all values of  $q$ . When  $s = N$ , the GVM reduces to the noiseless  $q$ -voter model [41, 47] on a fully-connected dyadic network. However, for networks that are not complete, the correspondence is not exact due to the explicit group constraint.

To clearly observe the effect of groups, consider the simplicial GVM. A basic property of voter dynamics is the exit time  $\tau$ , which is the time that it takes to reach consensus (towards either state) from a balanced initial condition (with the same number of nodes in each state). In Fig. 2, we show the exit time  $\tau$  for the simplicial GVM on “annealed” hypergraphs, in which the nodes of a hyperedge are determined randomly in each time step [54], with two different hyperedge-size distributions  $P(s)$  — a geometric distribution  $P(s) = [(\langle s \rangle - 2)/(\langle s \rangle - 1)]^{s-2}/(\langle s \rangle - 1)$  for  $s \geq 2$  and a power-law distribution  $P(s) = s^{-\alpha}/\sum_{\ell=2}^{\infty} \ell^{-\alpha}$  for  $s \geq 2$  — that are inspired by empirical hypergraph data sets [55–57]. We compute the exit time  $\tau$  as a function of the mean hyperedge size  $\langle s \rangle$  (for the geometric distribution) and the power-law exponent  $\alpha$  (for the power-law distribution) using Monte-Carlo (MC) simulations on hypergraphs with  $N = 10^5$  nodes. In both cases,  $\tau$  behaves nonmonotonically (see Fig. 2), so there are optimal values of  $\tau$ . As groups of three or more nodes begin to appear (i.e.,  $\langle s \rangle \gtrsim 2$  or  $\alpha < \infty$ ), consensus

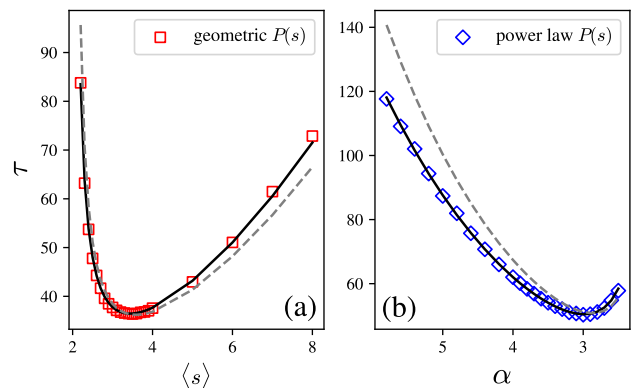


FIG. 2. The exit time  $\tau$  for the simplicial GVM on annealed hypergraphs with hyperedge sizes drawn from (a) a geometric distribution with different mean hyperedge sizes  $\langle s \rangle$  and (b) a power-law distribution with different power-law exponents  $\alpha$ . The symbols indicate the means of  $N = 10^3$  independent Monte-Carlo simulations with  $N = 10^5$  nodes, and the curves indicate analytical results from a recursion relation (solid) and a leading-order approximate solution (dotted) in the Supplemental Material (SM) [53]. Both situations exhibit the optimality: With increasing  $\langle s \rangle$  or decreasing  $\alpha$ , the exit time  $\tau$  first decreases but eventually increases, achieving a minimum in the middle.

accelerates (i.e.,  $\tau$  is smaller). However, when group sizes are too large (i.e.,  $\langle s \rangle \gg 2$  or  $\alpha \lesssim 3$ ), consensus decelerates. Therefore, there is an “optimal” level of group interactions that leads to the fastest consensus (i.e., the smallest  $\tau$ ).

To gain theoretical insight into the origin of this optimality, we analyze a generic version of the GVM, with duplicate choices allowed, on annealed  $s$ -uniform hypergraphs with  $N$  nodes. This setting admits a series of concrete, informative analytical results. In a uniform hypergraph, each hyperedge has the same size  $s$  (i.e., the same number of nodes). We consider the competition between our two independent parameters,  $q$  and  $s$ , in the opinion dynamics.

*Mean-field theory*—To theoretically understand the GVM dynamics, we use mean-field theory [37, 47]. A key variable is  $\rho(t)$ , which is the fraction of nodes of a hypergraph with state 1 at time  $t$ . In a time step,  $\rho(t)$  can increase or decrease by  $\delta\rho \equiv 1/N$ . One can account for this change with the transition probability  $R(\rho) \equiv P(\rho \rightarrow \rho + \delta\rho)$  that the number of nodes in state 1 increases by 1 in a time step and the transition probability  $L(\rho) \equiv P(\rho \rightarrow \rho - \delta\rho)$  for decreases by 1 in a time step. The probability of no change in  $\rho$  in one time step is  $1 - R(\rho) - L(\rho)$ . The rate equation for  $\rho(t)$  is then

$$\frac{d\rho}{dt} = R(\rho) - L(\rho) \equiv v(\rho), \quad (1)$$

where  $v(\rho)$  is the drift function.

For an annealed  $s$ -uniform hypergraph, one can write [53]

$$\begin{aligned}
 R(\rho) &= (1 - \rho) \sum_{n=0}^{s-1} \binom{s-1}{n} \rho^n (1 - \rho)^{s-1-n} \left( \frac{n}{s-1} \right)^q \\
 &= \frac{(1 - \rho)}{(s-1)^q} \left( \frac{d}{dr} \right)^q \left[ (1 - \rho + \rho e^r)^{s-1} \right] \Big|_{r=0}, \\
 L(\rho) &= \rho \sum_{n=0}^{s-1} \binom{s-1}{n} \rho^n (1 - \rho)^{s-1-n} \left( 1 - \frac{n}{s-1} \right)^q \\
 &= \frac{\rho}{(s-1)^q} \left( \frac{d}{dr} \right)^q \left[ (\rho + e^r - \rho e^r)^{s-1} \right] \Big|_{r=0}. \quad (2)
 \end{aligned}$$

In this mean-field approximation, the probability that a size- $s$  hyperedge has  $n$  nodes with state **1** at time  $t$  is  $\binom{s-1}{n} \rho^n (1 - \rho)^{s-1-n}$ .

The drift function  $v(\rho)$  gives many useful insights about GVM dynamics. When  $q = 1$  (i.e., for the standard VM),  $v(\rho) = 0$  for all  $\rho$  because  $R(\rho) = L(\rho) = \rho(1 - \rho)$  [37]. For the generic GVM (i.e., when  $q \geq 2$ ), the drift  $v(\rho)$  is no longer identically 0. We show in supplemental material (SM) [53] that Eq. (1) has three equilibrium points:  $\rho = 0$ ,  $\rho = 1$ , and  $\rho = 1/2$ . The equilibrium points  $\rho = 0$  and  $\rho = 1$  are stable and correspond to the consensus states with opinions **0** and **1**, respectively. Apart from finite-size fluctuations, the system eventually reaches the  $\rho = 0$  consensus equilibrium whenever  $\rho < 1/2$  because  $v(\rho) < 0$ . For  $\rho > 1/2$ , the system eventually reaches the consensus equilibrium  $\rho = 1$ . The unstable equilibrium point  $\rho = 1/2$  has an equal mixture of the opinions **0** and **1**. Drift towards a stable equilibrium point depends on the values of  $q$  and  $s$ , which thereby play crucial roles in the GVM dynamics. The drift function  $v(\rho)$  of the GVM for  $s = N$  reduces to that of the  $q$ -voter model on a fully-connected dyadic network [53].

*Sigmoidal exit probability*—Another key property of voter dynamics is the exit probability  $\Phi(\rho)$ , which is the probability to reach an opinion-1 consensus state from the initial density  $\rho$ . From the preceding argument, we expect that the exit probability for generic GVM (i.e., for any  $q \geq 2$ ) changes in a sigmoidal manner near  $\rho = 1/2$ , with convergence to a step function in the thermodynamic limit  $N \rightarrow \infty$ , as has also been observed in numerical simulations of the  $q$ -voter model [41]. To confirm this expectation and explicitly elucidate the group effect, we calculate  $\Phi(\rho)$  explicitly for large but finite  $N$ . Following [37], we set up the recursion relation

$$\begin{aligned}
 \Phi(\rho) &= R(\rho)\Phi(\rho + \delta\rho) + L(\rho)\Phi(\rho - \delta\rho) \\
 &\quad + [1 - R(\rho) - L(\rho)]\Phi(\rho) \quad (3)
 \end{aligned}$$

and Taylor-expand it in  $\delta\rho = 1/N$  to second order to obtain a backward Kolmogorov equation

$$v(\rho) \frac{\partial \Phi(\rho)}{\partial \rho} + D(\rho) \frac{\partial^2 \Phi(\rho)}{\partial \rho^2} = 0, \quad (4)$$

with a diffusion function  $D(\rho) \equiv [R(\rho) + L(\rho)]/(2N)$  and boundary conditions  $\Phi(0) = 0$  and  $\Phi(1) = 1$ . By symmetry,  $\Phi(1 - \rho) = 1 - \Phi(\rho)$ .

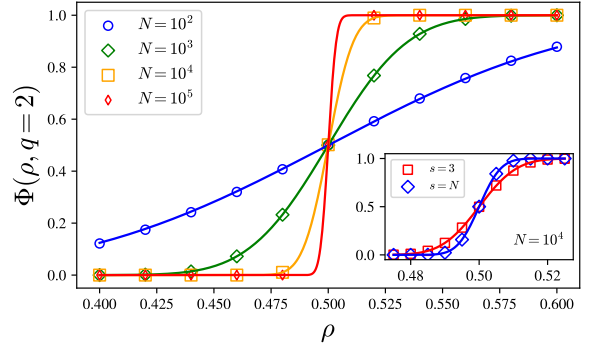


FIG. 3. The exit probability  $\Phi(\rho)$  when the nonlinearity strength is  $q = 2$  and the group size is  $s = 3$ . The solid curves are from the function in Eq. (5), and the markers are means of  $10^4$  independent MC simulations on annealed 3-uniform hypergraphs. As  $N$  increases, the sigmoid  $\Phi$  converges to a step function. In the inset, we show  $\Phi(\rho)$  for a fixed system size  $N$  and different group sizes  $s$ . Convergence to a step function is slower for  $s = 3$  than for  $s = N$ .

To illustrate the effect of the nonlinearity, we compare the two simplest cases:  $q = 1$  (i.e., the standard VM) and  $q = 2$  (our GVM). When  $q = 1$ , it is known that  $\Phi(\rho) = \rho$  [37], as one can view the dynamics as a diffusion process (i.e.,  $v(\rho) = 0$ ). For  $q = 2$ , we solve Eq. (4) explicitly to obtain [53]

$$\Phi(\rho) = \frac{1}{2} + \frac{\operatorname{erf} \left( \sqrt{\frac{2N(s-2)}{s}} \left( \rho - \frac{1}{2} \right) \right)}{2 \operatorname{erf} \left( \sqrt{\frac{N(s-2)}{2s}} \right)}, \quad (5)$$

where  $\operatorname{erf}(\cdot)$  is the error function. In Fig. 3, we plot  $\Phi(\rho)$  when  $q = 2$  with  $s = 3$ . It agrees with the results of our MC simulations. This explicit closed-form confirmation demonstrates that the “width”  $\Delta$  of the sigmoidal change across  $\rho = 1/2$  scales as  $\Delta \sim 1/\sqrt{N(s-2)/s}$ , illustrating both the finite-size effects (i.e., the dependence on  $N$ ) and the group effect (i.e., the dependence on  $s$ ). In particular, we see that convergence to a step function “slows down” for smaller group sizes  $s$  when  $q = 2$ . [See the inset of Fig. 3.]

*Logarithmic scaling of the exit time  $\tau$  with hypergraph size  $N$* —Following a similar procedure as in our derivation of Eq. (4) for the exit probability, we set up a recursion relation for the exit time  $T(\rho)$  from the initial density  $\rho$ . [Note that  $\tau \equiv T(\rho = 1/2)$ .] This yields the backward Kolmogorov equation [53]

$$v(\rho) \frac{\partial T(\rho)}{\partial \rho} + D(\rho) \frac{\partial^2 T(\rho)}{\partial \rho^2} = -1. \quad (6)$$

For the standard VM (i.e., for  $q = 1$ ), the drift term vanishes and we solve Eq. (6) and obtain  $T(\rho = 1/2) = N \ln 2$  [37]. However, for the GVM (i.e., for  $q \geq 2$ ), it is typically not possible to solve Eq. (6) analytically. Nonetheless, one can numerically solve the recursion relation for  $T(\rho)$  that is analogous to Eq. (3) [53].

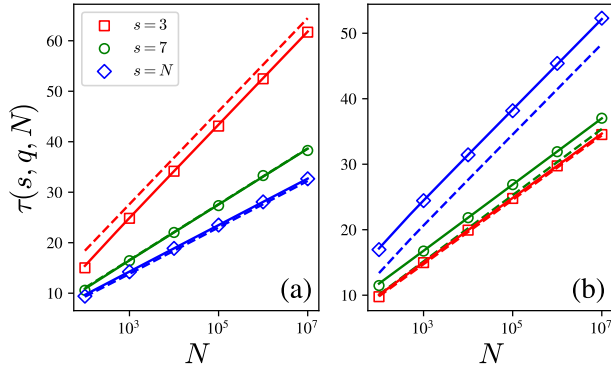


FIG. 4. Logarithmic scaling of the exit time  $\tau(s, q, N)$  on the hypergraph size  $N$  for (a) nonlinearity strength  $q = 2$  and (b) nonlinearity strength  $q = 5$ . The markers are means of  $10^6$  (when  $N \leq 10^4$ ) or  $10^3$  (when  $N \geq 10^5$ ) independent MC simulations on annealed  $s$ -uniform hypergraphs. The solid curves are from Eq. (6), and the dashed curves are from the leading-order solutions in Eqs. (8, 9). The dashed and solid green curves ( $s = 7$ ) in (a) nearly overlap.

To proceed further analytically, we approximate Eq. (6) by neglecting the diffusion term and then integrate to obtain the approximate exit time

$$\tau \equiv T(\rho = 1/2) \approx \int_{\frac{1}{2} - \frac{1}{\sqrt{N}}}^{\frac{1}{2}} \frac{1}{v(\rho')} d\rho'. \quad (7)$$

We have shifted the initial density by  $1/\sqrt{N}$  from  $1/2$  to exploit intrinsic stochasticity and thereby avoid being trapped at the unstable equilibrium point. Under this approximation, we obtain to the leading order in the hypergraph size  $N$  that  $\tau(N; s, q) \sim \mathcal{A}(s, q) \ln N$ , where the prefactor  $\mathcal{A}(s, q)$  depends on  $s$  and  $q$  for general  $q \geq 2$  and  $s \geq 3$  [see Eq. (S32) in the SM [53]]. One can attribute the logarithmic scaling of the exit time of the generic GVM to the property of the drift function  $v(\rho)$  that  $v(\rho) = 0$  has three simple roots in  $[0, 1]$ . The prefactor  $\mathcal{A}(s, q)$  diverges for  $s = 2$ , as  $\tau$  satisfies diffusive scaling  $\tau \sim \mathcal{O}(N)$  for dyadic networks.

It is insightful to show some explicit approximate solutions of  $\tau$ . For example, as depicted in Fig. 4, the leading-order expression of  $\tau$  for  $q = 2$  and  $q = 5$  are [53]

$$\tau(N, s; q = 2) \sim \frac{2(s-1)}{(s-2)} \ln N, \quad (8)$$

$$\tau(N, s; q = 5) \sim \frac{(s-1)^4 (3s-4)(s+1)}{s(s-2)(s^2-2s+2)} \ln N. \quad (9)$$

From Fig. 4, we see that the analytically-obtained logarithmic scaling of  $\tau$  successfully explains the MC simulation results. Figure 4 also reveals that the group effect can manifest distinctively for different nonlinearity strengths  $q$ . When  $q = 2$ , reaching consensus takes the longest time for the smallest group size  $s = 3$  [see Fig. 4(a)]. By contrast, when  $q = 5$ , the longest consensus time occurs for the largest group size  $s = N$  [see Fig. 4(b)].

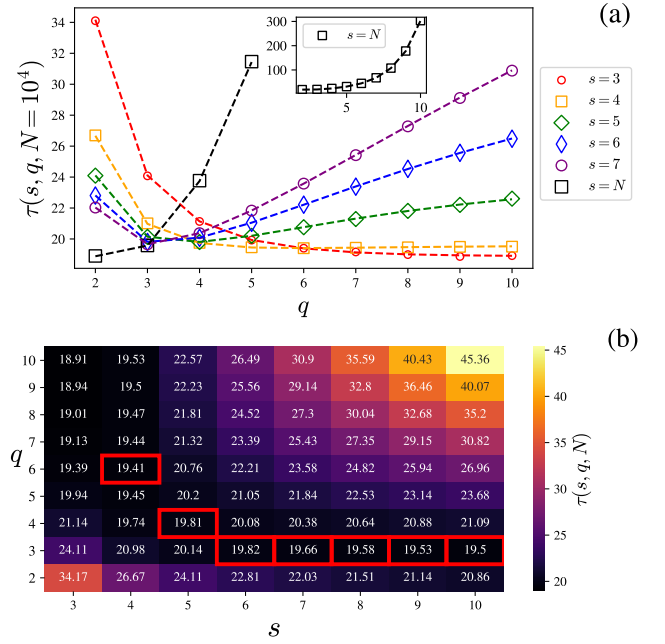


FIG. 5. (a) The dependence on the nonlinearity strength  $q$  of the exit time  $\tau$  for different values of the group size  $s$  for hypergraphs with  $N = 10^4$  nodes. The markers are means of  $10^4$  independent MC simulations on annealed  $s$ -uniform hypergraphs, and the analytical curves are from numerical solutions of the recursion relation. When  $s = N$ , the exit time  $\tau$  grows exponentially quickly with  $q$ , making it problematic to depict it along with other cases. In the inset, we show the result for  $s = N$  in an extended  $q$  range. (b) The heatmap for  $\tau(s, q, N)$  that we obtain from numerical solutions of the recursion relation with  $N = 10^4$ . For a given  $s$ , the cell with the red border has the optimal  $\tau$ .

*Optimality in the exit time  $\tau$* —To further examine the complex interplay between the nonlinearity and group effect on the exit time  $\tau$ , we investigate how varying nonlinearity strength  $q$  affects the GVM dynamics for specified values of the group size  $s$  and hypergraph size  $N$ . In the absence of the group constraint (i.e.,  $s = N$ ), the leading-order expression of the exit time  $\tau$  is

$$\tau(q; N, s = N) \sim \left(1 + \frac{2^{q-2}}{q-1}\right) \ln N. \quad (10)$$

This expression also applies to the  $q$ -voter model on a complete dyadic graph. Because  $\tau$  increases with  $q$ , a stronger nonlinearity decelerates consensus [see Fig. 5(a) and its inset]. By contrast, with the most-constraining groups (i.e.,  $s = 3$ ),  $\tau$  decreases monotonically with  $q$ . To leading order,  $\tau(q; N, s = 3) \sim \frac{2^q}{2^{2q-1}-1} \ln N$ . A stronger nonlinearity accelerates consensus [see Fig. 5(a), red].

There is a nontrivial tradeoff between these extreme situations. As we can see in Fig. 5(a), for a given hyperedge size  $s$ , there is an optimal nonlinearity strength  $q^*$  with the minimum exit time  $\tau$ . We systematically investigate the tradeoff for many values of  $s$  and  $q$  [see Fig. 5(b)]. These computations reveal the global landscape of GVM dynamics and the associated geography of optimality.



We now explain why we observe optimality. From the inset of Fig. 5(a), we see that considering the opinions of exactly 2 neighbors is the most efficient way to achieve consensus. Increasing  $q$  in Eq. (10) with  $s = N$  reduces the probability that neighbors have unanimous opinions, which decreases the value of the drift function  $v(\rho)$  and decelerates the approach to consensus. As  $q$  grows logarithmically with  $N$  [i.e.,  $q \sim \mathcal{O}(\ln N)$ ], the logarithmic scaling of  $\tau$  in Eq. (10) eventually becomes a linear scaling  $\tau \sim \mathcal{O}(N)$ , which is comparable to the diffusive scaling for  $q = 1$ . Moreover, when  $s$  is finite, the probability that a node consults the same neighbor twice (instead of consulting 2 different neighbors) for  $q = 2$  is  $1/(s - 1)$ , which is nonnegligible for small  $s$ . In this situation, a node only consults the opinion of 1 neighbor, so it again effectively follows diffusive dynamics. More generally, the probability of diffusive dynamics from consulting just 1 neighbor increases with decreasing  $q$ . Therefore, there is a “sweet spot”  $q^*$  that minimizes  $\tau$  when  $2 < q^* < \mathcal{O}(\ln N)$  between the two diffusive-dynamics maxima. The case of  $s = 3$  is notable exception to this; the maximum number of different neighbors is 2, so  $\tau$  decreasing indefinitely (although slowly) as  $q$  increases.

We can also explain the presence of optimality in the simplicial GVM in Fig. 2 as a competition between the diffusive dynamics from dyadic edges (which dominates as  $\langle s \rangle \downarrow 2$  and  $\alpha \rightarrow \infty$ ) and the small probability of unanimity in large hyperedges (which dominates as  $\langle s \rangle \rightarrow \infty$  and  $\alpha \downarrow 2$ ). Following the same logic as above, we again obtain an optimum in the opinion dynamics.

**Conclusions**—We formulated and analyzed a group-driven voter model (GVM) that accounts for the effects of both polyadic and nonlinear interactions within groups. A larger nonlinearity strength  $q$  leads to faster consensus in the GVM than in conventional VMs, which exhibit diffusive dynamics. This acceleration of consensus formation depends on the interplay between the nonlinearity strength  $q$  and the group size  $s$  of hypergraphs. Through mean-field calculations and Monte-Carlo simulations, we demonstrated that the exit time scales logarithmically with system size and that there is an optimum value  $q^*$  of the nonlinearity strength  $q$  that minimizes the exit time. This optimality emerges from a competition between diffusive dynamics when both  $q$  and  $s$  are small and a slow drift when both  $q$  and  $s$  are large. This emergent group effect cannot arise in dyadic networks, providing justification for the analysis of dynamics on polyadic networks.

We also apply our analytical approach to several variants of our GVM (see the SM [53]): the simplicial GVM, the GVM without allowing duplicate choices, and a GVM with edge-update dynamics in which we simultaneously update the opinions of all nodes that are attached to a hyperedge. In all of these cases, the exit time scales logarithmically with system size, illustrating the robustness of our main theoretical results [53].

**Acknowledgments**—We thank Sid Redner for useful conversations and suggestions. This work was supported in part by National Research Foundation

of Korea (NRF) grants funded by the Korea government (MSIT) [No. 2020R1A2C2003669 (K-IG) and No. 2020R1I1A3068803 (BM)]; by a KIAS Individual Grant [No. CG079902] at Korea Institute for Advanced Study (D-SL); by the National Science Foundation (grant number 1922952) through their program on Algorithms for Threat Detection (MAP); and by Agencia Estatal de Investigación (AEI, MCI, Spain) MCIN/AEI/10.13039/501100011033 and Fondo Europeo de Desarrollo Regional (FEDER, UE) under Projects APASOS [PID2021-122256NB-C21] and the Maria de Maeztu Program for Units of Excellence in R&D grant [CEX2021-001164-M] (MSM).

---

\* deoksunlee@kias.re.kr

† bmin@cbnu.ac.kr

‡ mason@math.ucla.edu

§ maxi@ifisc.uib-csic.es

¶ kgoh@korea.ac.kr

- [1] D. W. Olmsted, *Sociol. Quart.* **3**, 195 (1962).
- [2] S. A. Wheelan, *Group Processes: A Developmental Perspective* (Allyn & Bacon, Boston, MA, USA, 1994).
- [3] T. Tyson, *Working with Groups* (Macmillan Publishers, London, UK, 1998).
- [4] R. Brown and S. Pehrson, *Group Processes: Dynamics Within and Between Groups* (John Wiley & Sons, Hoboken, NJ, USA, 2019).
- [5] C. Bick, E. Gross, H. A. Harrington, and M. T. Schaub, *SIAM Rev.* **65**, 686 (2023).
- [6] F. Battiston, G. Cencetti, I. Iacopini, V. Latora, M. Lucas, A. Patania, J.-G. Young, and G. Petri, *Phys. Rep.* **874**, 1 (2020).
- [7] G. Bianconi, *Higher-Order Networks* (Cambridge University Press, Cambridge, UK, 2021).
- [8] S. Boccaletti, P. De Lellis, C. del Genio, K. Alfaro-Bittner, R. Criado, S. Jalan, and M. Romance, *Phys. Rep.* **1018**, 1 (2023).
- [9] S. Majhi, M. Perc, and D. Ghosh, *J. R. Soc. Interface* **19**, 20220043 (2022).
- [10] I. Iacopini, G. Petri, A. Barrat, and V. Latora, *Nat. Commun.* **10**, 2085 (2019).
- [11] P. S. Skardal and A. Arenas, *Phys. Rev. Lett.* **122**, 248301 (2019).
- [12] G. St-Onge, A. Allard, L. Hébert-Dufresne, and G. Bianconi, *Phys. Rev. Lett.* **127**, 158301 (2021).
- [13] G. St-Onge, I. Iacopini, V. Latora, A. Barrat, G. Petri, A. Allard, and L. Hébert-Dufresne, *Comm. Phys.* **5**, 25 (2022).
- [14] G. F. de Arruda, G. Petri, P. M. Rodriguez, and Y. Moreno, *Nat. Commun.* **14**, 1375 (2023).
- [15] T. Carletti, L. Giambagli, and G. Bianconi, *Phys. Rev. Lett.* **130**, 187401 (2023).
- [16] G. Cencetti, D. A. Contreras, M. Mancastroppa, and A. Barrat, *Phys. Rev. Lett.* **130**, 247401 (2023).
- [17] J. Kim, D.-S. Lee, and K.-I. Goh, *Phys. Rev. E* **108**, 034313 (2023).
- [18] G. Burgio, S. Gómez, and A. Arenas, *Phys. Rev. Lett.* **132**, 077401 (2024).
- [19] J.-H. Kim and K.-I. Goh, *Phys. Rev. Lett.* **132**, 087401 (2024).
- [20] A. Civilini, O. Sadekar, F. Battiston, J. Gómez-Gardeñes, and V. Latora, *Phys. Rev. Lett.* **132**, 167401 (2024).
- [21] R. Sahasrabudhe, L. Neuhäuser, and R. Lambiotte, *J. Phys.*

- Complex. **2**, 025006 (2021).
- [22] J. Noonan and R. Lambiotte, Phys. Rev. E **104**, 024316 (2021).
- [23] H. Schawe and L. Hernández, Commun. Phys. **5**, 32 (2022).
- [24] A. Hickok, Y. Kureh, H. Z. Brooks, M. Feng, and M. A. Porter, SIAM J. Appl. Dyn. Syst. **21**, 1 (2022).
- [25] L. Horstmeyer and C. Kuehn, Phys. Rev. E **101**, 022305 (2020).
- [26] N. Papanikolaou, G. Vaccario, E. Hormann, R. Lambiotte, and F. Schweitzer, Phys. Rev. E **105**, 054307 (2022).
- [27] T. M. Liggett, *Stochastic Interacting Systems: Contact, Voter and Exclusion Processes* (Springer-Verlag, Heidelberg, Germany, 1999).
- [28] C. Castellano, S. Fortunato, and V. Loreto, Rev. Mod. Phys. **81**, 591 (2009).
- [29] P. L. Krapivsky, S. Redner, and E. Ben-Naim, *A Kinetic View of Statistical Physics* (Cambridge University Press, Cambridge, UK, 2010).
- [30] I. Dornic, H. Chaté, J. Chave, and H. Hinrichsen, Phys. Rev. Lett. **87**, 045701 (2001).
- [31] There are several variants of “the” VM, depending on choices such as whether one selects nodes or edges at random, that have different qualitative dynamics [40].
- [32] R. A. Holley and T. M. Liggett, Ann. Prob. **3**, 643 (1975).
- [33] C. Castellano, D. Vilone, and A. Vespignani, Europhys. Lett. **63**, 153 (2003).
- [34] K. Suchecki, V. M. Eguíluz, and M. San Miguel, Europhys. Lett. **69**, 228 (2005).
- [35] V. Sood and S. Redner, Phys. Rev. Lett. **94**, 178701 (2005).
- [36] F. Vazquez, V. M. Eguíluz, and M. San Miguel, Phys. Rev. Lett. **100**, 108702 (2008).
- [37] V. Sood, T. Antal, and S. Redner, Phys. Rev. E **77**, 041121 (2008).
- [38] F. Vazquez and V. M. Eguíluz, New J. Phys. **10**, 063011 (2008).
- [39] N. Masuda, Phys. Rev. E **90**, 012802 (2014).
- [40] S. Redner, C. R. Phys. **20**, 275 (2019).
- [41] C. Castellano, M. A. Muñoz, and R. Pastor-Satorras, Phys. Rev. E **80**, 041129 (2009).
- [42] D. Centola and M. W. Macy, Am. J. Sociol. **113**, 702 (2007).
- [43] A. Nowak, J. Szamrej, and B. Latané, Psychol. Rev. **97**, 362 (1990).
- [44] R. Lambiotte and S. Redner, J. Stat. Mech. **2007**, L10001 (2007).
- [45] D. Volovik and S. Redner, J. Stat. Mech. **2012**, P04003 (2012).
- [46] Y. H. Kureh and M. A. Porter, Phys. Rev. E **101**, 062303 (2020).
- [47] L. S. Ramirez, F. Vazquez, M. San Miguel, and T. Galla, Phys. Rev. E **103**, 034307 (2024).
- [48] M. Bond, *The Power of Others: Peer Pressure, Groupthink, and How the People Around Us Shape Everything We Do* (Simon and Schuster, New York, NY, USA, 2014).
- [49] Z. Ruan, G. Iniguez, M. Karsai, and J. Kertész, Phys. Rev. Lett. **115**, 218702 (2015).
- [50] J. S. Juul and M. A. Porter, Chaos **28**, 013115 (2018).
- [51] L. Neuhäuser, A. Mellor, and R. Lambiotte, Phys. Rev. E **101**, 032310 (2020).
- [52] A. Jedrzejewski and K. Sznajd-Weron, C. R. Phys. **20**, 244 (2019).
- [53] See the Supplemental Material for details.
- [54] M. Boguñá, C. Castellano, and R. Pastor-Satorras, Phys. Rev. E **79**, 036110 (2009).
- [55] A. Patania, G. Petri, and F. Vaccarino, EPJ Data Sci. **6**, 18 (2017).
- [56] A. R. Benson, R. Abebe, M. T. Schaub, A. Jadbabaie, and J. Kleinberg, Proc. Natl. Acad. Sci. USA **115**, E11221 (2018).
- [57] D. Roh and K.-I. Goh, J. Korean Phys. Soc. **83**, 713 (2023).

# Supplemental Material for “Competition between group interactions and nonlinearity in voter dynamics on hypergraphs”

Jihye Kim,<sup>1,2</sup> Deok-Sun Lee,<sup>2,3,\*</sup> Byunghoon Min,<sup>4,†</sup> Mason A. Porter,<sup>5,6,7,‡</sup> Maxi San Miguel,<sup>8,§</sup> and K.-I. Goh<sup>1,5,¶</sup>

<sup>1</sup>*Department of Physics, Korea University, Seoul 02841, Korea*

<sup>2</sup>*School of Computational Sciences, Korea Institute for Advanced Study, Seoul 02455, Korea*

<sup>3</sup>*Center for AI and Natural Sciences, Korea Institute for Advanced Study, Seoul 02455, Korea*

<sup>4</sup>*Department of Physics, Chungbuk National University, Cheongju, Chungbuk 28644, Korea*

<sup>5</sup>*Department of Mathematics, University of California, Los Angeles, Los Angeles, CA 90095, USA*

<sup>6</sup>*Department of Sociology, University of California, Los Angeles, Los Angeles, CA 90095, USA*

<sup>7</sup>*Santa Fe Institute, Santa Fe, NM 87501, USA*

<sup>8</sup>*Instituto de Física Interdisciplinar y Sistemas Complejos, IFISC (CSIC-UIB),  
Campus Universitat Illes Balears, E-07122 Palma de Mallorca, Spain*

This Supplemental Material for “Competition between group interactions and nonlinearity in voter dynamics on hypergraphs” consists of three major sections.

## CONTENTS

S1. Monte-Carlo simulations of our GVM	1
A. Simplicial GVM on annealed hypergraphs	1
B. GVM on annealed $s$ -uniform hypergraphs	2
S2. Detailed derivations of our main analytical results	2
A. Transition probabilities for general $P(s)$	2
B. Derivation of the exit probability $\Phi(\rho)$	4
C. Derivations of the exit times $T(\rho)$ and $\tau \equiv T(\rho = 1/2)$	5
1. Numerical solution of the recursion relation (S20)	5
2. Derivation of the logarithmic scalings of $T(\rho)$ and $\tau$	6
3. Explicit derivation of the formulas for $\tau$ in the main manuscript	7
4. Dependence of the exit time $T(\rho_0)$ on the initial density $\rho_0$	8
S3. Variants of our GVM	9
A. Simplicial GVM	9
B. GVM without duplicate selections	10
C. GVM with edge-update dynamics	10
References	13

## S1. MONTE-CARLO SIMULATIONS OF OUR GVM

We now provide algorithmic details of the employed Monte-Carlo (MC) simulations. The codes associated with this paper are publicly available via GitHub at <https://github.com/JihyeKim2024/GVM>.

### A. Simplicial GVM on annealed hypergraphs

In Fig. 2 of the main manuscript, we showed results of MC simulations for the simplicial GVM on annealed hypergraphs with  $N$  nodes and hyperedge-size distribution  $P(s)$ . In an annealed hypergraph, the elements of a hyperedge are not fixed (i.e., “quenched”); instead, we determine them randomly at each time step. For an annealed hypergraph with hyperedge-size distribution  $P(s)$ , each MC step has the following three stages:

\* deoksunlee@kias.re.kr

† bmin@cbnu.ac.kr

‡ mason@math.ucla.edu

§ maxi@ifisc.uib-csic.es

¶ kgoh@korea.ac.kr

- (i) We select a node  $v$  uniformly at random with probability  $1/N$ .
- (ii) We draw a random number  $s$  from the probability distribution  $sP(s)/\langle s \rangle$ , where  $\langle s \rangle = \sum_{s=2}^{\infty} sP(s)$  is the mean hyperedge size. We then select  $s - 1$  distinct nodes uniformly at random of the  $N - 1$  other nodes (i.e., excluding  $v$  itself) of the hypergraph to form a hyperedge  $h$ .
- (iii) The node  $v$  flips its state  $\sigma_v$  if and only if the states of all  $s - 1$  other nodes in the selected hyperedge  $h$  are unanimously different from  $\sigma_v$ .

### B. GVM on annealed $s$ -uniform hypergraphs

In Figs. 3–5 of the main manuscript, we showed results of MC simulations of the GVM on annealed  $s$ -uniform hypergraphs with  $N$  nodes. An  $s$ -uniform hypergraph is a hypergraph in which every hyperedge has the same cardinality (i.e., size)  $s$ . For the GVM on an annealed  $s$ -uniform hypergraph, each MC step has the following three stages:

- (i) We select a node  $v$  uniformly at random with probability  $1/N$ .
- (ii) We select  $s - 1$  distinct nodes uniformly at random from the other  $N - 1$  nodes (i.e., excluding  $v$  itself) of the hypergraph to form a hyperedge  $h$ .
- (iii) We select a node other than  $v$  from the hyperedge  $h$  uniformly at random from the  $s - 1$  remaining nodes, and we record the state  $\sigma$  of this node. We repeat this process  $q - 1$  times for a total of  $q$  independent instances of this process. The node  $v$  flips its state  $\sigma_v$  if and only if the  $q$  states are unanimously different from  $\sigma_v$ .

In stage (iii), one may or may not allow duplicate selections of the same neighboring node. The GVM in the main manuscript does allow duplicate selections. In Sec. S3 B, we consider a variant of our GVM in which we do not allow duplicate selections.

## S2. DETAILED DERIVATIONS OF OUR MAIN ANALYTICAL RESULTS

In this section, we give detailed derivations of our main analytical results for the GVM in the main manuscript. In this GVM, a node consults  $q$  neighboring opinions with duplicate selections allowed.

### A. Transition probabilities for general $P(s)$

To track the time evolution of the fraction  $\rho(t)$  of nodes in state **1** at time  $t$  in a hypergraph, we consider the transition probabilities  $R(\rho) \equiv P(\rho \rightarrow \rho + 1/N)$  (i.e., the “raising operator”) and  $L(\rho) \equiv P(\rho \rightarrow \rho - 1/N)$  (i.e., the “lowering operator”) [S1]. The probability that a selected hyperedge in stage (ii) has size  $s$  is proportional to  $sP(s)$ , so the mean-field expression for the raising operator  $R(\rho)$  is

$$\begin{aligned} R(\rho) &= \frac{(1-\rho)}{\sum_s sP(s)} \sum_s sP(s) \sum_{n=1}^{s-1} \frac{(s-1)!}{n!(s-1-n)!} \rho^n (1-\rho)^{s-1-n} \left(\frac{n}{s-1}\right)^q \\ &= \frac{\rho(1-\rho)}{\sum_s sP(s)} \sum_s sP(s) R_s(\rho), \end{aligned} \quad (\text{S1})$$

where

$$R_s(\rho) = \sum_{n=1}^{s-1} \frac{(s-2)!}{(n-1)!(s-1-n)!} \rho^{n-1} (1-\rho)^{s-1-n} \left(\frac{n}{s-1}\right)^{q-1}. \quad (\text{S2})$$

For an annealed  $s$ -uniform hypergraph, Eq. (S1) reduces to Eq. (2) of the main manuscript.

We proceed by expressing Eq. (S2) in terms of  $\rho$ ,  $s$ , and  $q$  using the relation

$$n^{q-1} = 1 + \sum_{r=1}^{q-1} A_{r,q} \prod_{l=1}^r (n-l), \quad (\text{S3})$$



with positive integers  $A_{r,q} \equiv \left[ \frac{(r+1)^{q-1} - r^q + r - 1}{r!} + \mathbf{1}_{r \geq 3} \sum_{l=2}^{r-1} \frac{(r-l+1)^{q-1} - 1}{l!(r-l)!} (-1)^l \right]$ , where the indicator symbol  $\mathbf{1}_{r \geq 3}$  has the value 1 when  $r \geq 3$  and 0 otherwise. Note that  $A_{r,q} = 0$  for  $r \geq q$  and that  $A_{q-1,q} = 1$ . Inserting Eq. (S3) into Eq. (S2) yields

$$\begin{aligned}
R_s(\rho) &= \frac{1}{(s-1)^{q-1}} \left[ 1 + \sum_{n=1}^{s-1} \sum_{r=1}^{q-1} \frac{(s-2)!}{(n-1)!(s-1-n)!} \rho^{n-1} (1-\rho)^{s-1-n} A_{r,q} \prod_{l=1}^r (n-l) \right] \\
&= \frac{1}{(s-1)^{q-1}} + \frac{1}{(s-1)^{q-1}} \sum_{n=2}^{s-1} A_{1,q} \frac{\rho(s-2)(s-3)!}{(n-2)!(s-1-n)!} \rho^{n-2} (1-\rho)^{s-1-n} \\
&\quad + \frac{1}{(s-1)^{q-1}} \sum_{n=3}^{s-1} A_{2,q} \frac{\rho^2(s-2)(s-3)(s-4)!}{(n-3)!(s-1-n)!} \rho^{n-3} (1-\rho)^{s-1-n} + \dots \\
&\quad + \frac{1}{(s-1)^{q-1}} \sum_{n=q}^{s-1} A_{q-1,q} \frac{\rho^{q-1}(s-q-1)! \prod_{l=1}^{q-1} (s-1-l)}{(n-q)!(s-1-n)!} \rho^{n-q} (1-\rho)^{s-1-n} \\
&= \frac{1}{(s-1)^{q-1}} \left[ 1 + A_{1,q} \rho(s-2) + A_{2,q} \rho^2(s-2)(s-3) + \dots + A_{q-1,q} \rho^{q-1} \prod_{l=1}^{q-1} (s-1-l) \right] \\
&= \frac{1}{(s-1)^{q-1}} \left[ 1 + \sum_{r=1}^{q-1} A_{r,q} \rho^r \prod_{l=1}^r (s-1-l) \right]. \tag{S4}
\end{aligned}$$

Therefore,

$$R(\rho) = \frac{\rho(1-\rho)}{\sum_s sP(s)} \sum_s \frac{sP(s)}{(s-1)^{q-1}} \left[ 1 + \sum_{r=1}^{q-1} A_{r,q} \rho^r \prod_{l=1}^r (s-1-l) \right]. \tag{S5}$$

When  $q \geq s$ , the leading term in the square brackets of Eq. (S5) is  $A_{s-2,q} \rho^{s-2} (s-2)!$ .

The lowering operator  $L(\rho)$  satisfies  $L(\rho) = R(1-\rho)$ , so

$$L(\rho) = \frac{\rho(1-\rho)}{\sum_s sP(s)} \sum_s \frac{sP(s)}{(s-1)^{q-1}} \left[ 1 + \sum_{r=1}^{q-1} A_{r,q} (1-\rho)^r \prod_{l=1}^r (s-1-l) \right]. \tag{S6}$$

We illustrate some explicit formulas for  $R(\rho)$  using Eq. (S5) for a few specific parameter choices:

$$\begin{aligned}
R(\rho) &= \rho(1-\rho) \quad \text{for either } q = 1 \text{ or } s = 2, \\
R(\rho) &= \frac{\rho(1-\rho)}{(s-1)} [1 + (s-2)\rho] \quad \text{for } q = 2, \\
R(\rho) &= \frac{\rho(1-\rho)}{(s-1)^2} [1 + 3(s-2)\rho + (s-2)(s-3)\rho^2] \quad \text{for } q = 3, \\
R(\rho) &= \frac{\rho(1-\rho)}{(s-1)^3} [1 + 7(s-2)\rho + 6(s-2)(s-3)\rho^2 + (s-2)(s-3)(s-4)\rho^3] \quad \text{for } q = 4, \text{ and} \\
R(\rho) &= \frac{\rho(1-\rho)}{(s-1)^{q-1}} \left[ 1 + \sum_{r=1}^{s-2} A_{r,q} \rho^r \prod_{l=1}^r (s-1-l) \right] \quad \text{for } q \rightarrow \infty. \tag{S7}
\end{aligned}$$

In Fig. S1(a), we show the drift function  $v(\rho) \equiv R(\rho) - L(\rho) = R(\rho) - R(1-\rho)$  from Eq. (S7) for  $s = 7$ .

When  $s = N \gg 1$ , the raising operator  $R(\rho)$  converges to

$$R(\rho) = (1-\rho)\rho^q, \tag{S8}$$

which leads to the drift function

$$v(\rho) \equiv R(\rho) - L(\rho) = (1-\rho)\rho^q - \rho(1-\rho)^q, \tag{S9}$$

which corresponds to Eq. (10) of Ref. [S2]. In Fig. S1(b), we plot  $v(\rho)$  from Eq. (S9) for  $s = N$ .

When either  $q = 1$  or  $s = 2$ , we have  $R(\rho) = L(\rho) = \rho(1-\rho)$ , which implies that the drift function  $v(\rho) = 0$ . The dynamics becomes purely diffusive, as in Ref. [S1]. Hereafter, unless we note otherwise, we thus focus our analysis on the cases  $q \geq 2$  and  $s \geq 3$ .

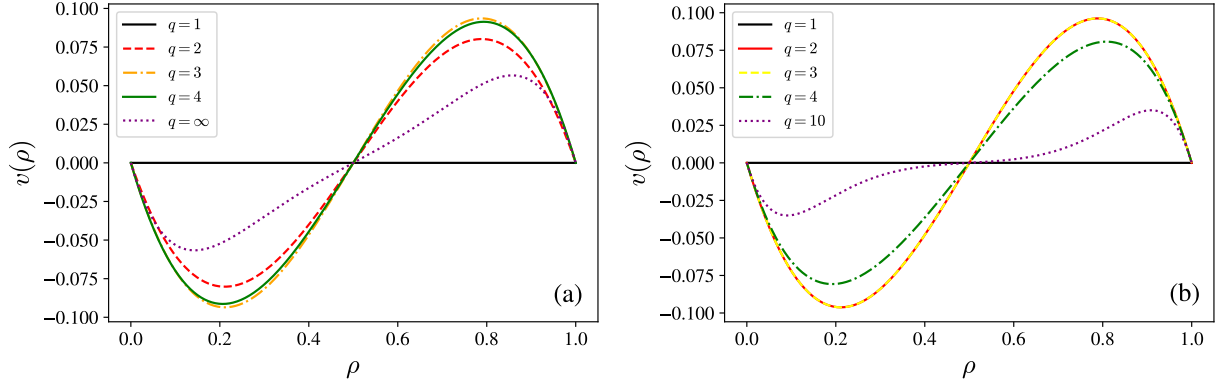


FIG. S1. The drift function  $v(\rho) = R(\rho) - L(\rho)$  for different values of  $q$  when (a)  $s = 7$  and (b)  $s = N$ . The curves for  $q = 2$  and  $q = 3$  in (b) completely overlap.

### B. Derivation of the exit probability $\Phi(\rho)$

The exit probability  $\Phi(\rho)$  satisfies the recursion relation

$$\Phi(\rho) = R(\rho)\Phi(\rho + \delta\rho) + L(\rho)\Phi(\rho - \delta\rho) + [1 - R(\rho) - L(\rho)]\Phi(\rho), \quad (\text{S10})$$

which is Eq. (3) of the main manuscript. We Taylor-expand  $\Phi(\rho \pm \delta\rho)$  in  $\delta\rho$  up to second order and write

$$\Phi(\rho \pm \delta\rho) \approx \Phi(\rho) \pm \frac{\partial\Phi(\rho)}{\partial\rho}\delta\rho + \frac{1}{2}\frac{\partial^2\Phi(\rho)}{\partial\rho^2}(\delta\rho)^2. \quad (\text{S11})$$

We then substitute Eq. (S11) into Eq. (S10) to obtain the backward Kolmogorov equation

$$v(\rho)\frac{\partial\Phi(\rho)}{\partial\rho} + D(\rho)\frac{\partial^2\Phi(\rho)}{\partial\rho^2} = 0, \quad (\text{S12})$$

where  $v(\rho) \equiv R(\rho) - L(\rho)$  and  $D(\rho) \equiv [R(\rho) + L(\rho)]/(2N)$ . From Eqs. (S5) and (S6),  $v(\rho)$  and  $D(\rho)$  are given by

$$v(\rho) = \frac{\rho(1-\rho)}{\sum_s sP(s)} \sum_s \frac{sP(s)}{(s-1)^{q-1}} \sum_{r=1}^{q-1} A_{r,q} [\rho^r - (1-\rho)^r] \prod_{l=1}^r (s-1-l) \quad (\text{S13})$$

and

$$D(\rho) = \frac{1}{2N} \frac{\rho(1-\rho)}{\sum_s sP(s)} \sum_s \frac{sP(s)}{(s-1)^{q-1}} \left\{ 2 + \sum_{r=1}^{q-1} A_{r,q} [\rho^r + (1-\rho)^r] \prod_{l=1}^r (s-1-l) \right\}. \quad (\text{S14})$$

We now obtain an explicit expression for  $\Phi(\rho)$  for the GVM with  $q = 2$  on an annealed  $s$ -uniform hypergraph. In this case, the raising and lowering operators are

$$\begin{aligned} R(\rho) &= \frac{\rho(1-\rho)}{(s-1)} [1 + (s-2)\rho], \\ L(\rho) &= \frac{\rho(1-\rho)}{(s-1)} [1 + (s-2)(1-\rho)], \end{aligned} \quad (\text{S15})$$

which implies that

$$\begin{aligned} v(\rho) &= \frac{(s-2)}{(s-1)} \rho(1-\rho)(2\rho-1), \\ D(\rho) &= \frac{1}{2N} \frac{s}{(s-1)} \rho(1-\rho). \end{aligned} \quad (\text{S16})$$

We write the derivative of  $\Phi(\rho)$  with respect to  $\rho$  as  $\exp[-f(\rho)]$ , where

$$\begin{aligned} f(\rho) &= \int \frac{v(\rho)}{D(\rho)} d\rho \\ &= \int \frac{2N(s-2)(2\rho-1)}{s} d\rho \\ &= \frac{N(s-2)}{2s} - \frac{2N(s-2)(\rho-1/2)^2}{s}. \end{aligned} \quad (\text{S17})$$

Using the boundary conditions  $\Phi(0) = 0$  and  $\Phi(1) = 1$ , we obtain

$$\Phi(\rho) = \frac{\int_0^\rho \exp\left[\frac{-2N(s-2)(\rho'-1/2)^2}{s}\right] d\rho'}{\int_0^1 \exp\left[\frac{-2N(s-2)(\rho'-1/2)^2}{s}\right] d\rho'} = \frac{\int_{-\frac{N(s-2)}{2s}}^{\frac{N(s-2)(\rho-1/2)}{2s}} \exp[-y^2] dy}{\int_{-\frac{N(s-2)}{2s}}^{\frac{N(s-2)}{2s}} \exp[-y^2] dy}, \quad (\text{S18})$$

where  $y = \sqrt{2N(s-2)/s}(\rho-1/2)$ . This yields Eq. (5) of the main manuscript:

$$\Phi(\rho) = \frac{1}{2} + \frac{\operatorname{erf}\left(\sqrt{\frac{2N(s-2)}{s}}\left(\rho - \frac{1}{2}\right)\right)}{2 \operatorname{erf}\left(\sqrt{\frac{N(s-2)}{2s}}\right)}, \quad (\text{S19})$$

where  $\operatorname{erf}(x) \equiv 2 \int_0^x \exp[-z^2] dz / \sqrt{\pi}$  is the error function.

### C. Derivations of the exit times $T(\rho)$ and $\tau \equiv T(\rho = 1/2)$

The exit time  $T(\rho)$  satisfies the recursion relation

$$T(\rho) = R(\rho)T(\rho + \delta\rho) + L(\rho)T(\rho - \delta\rho) + [1 - R(\rho) - L(\rho)]T(\rho) + \delta t, \quad (\text{S20})$$

with  $\delta t = 1/N$ . We Taylor-expand  $T(\rho \pm \delta\rho)$  in  $\delta\rho$  up to second order and write

$$T(\rho \pm \delta\rho) \approx T(\rho) \pm \frac{\partial T(\rho)}{\partial \rho} \delta\rho + \frac{1}{2} \frac{\partial^2 T(\rho)}{\partial \rho^2} (\delta\rho)^2, \quad (\text{S21})$$

which we insert into Eq. (S20) to obtain the backward Kolmogorov equation

$$v(\rho) \frac{\partial T(\rho)}{\partial \rho} + D(\rho) \frac{\partial^2 T(\rho)}{\partial \rho^2} = -1, \quad (\text{S22})$$

which is Eq. (6) of the main manuscript.

#### 1. Numerical solution of the recursion relation (S20)

It is challenging to obtain an exact analytical solution of Eq. (S22), so we compute  $T(\rho)$  by numerically solving Eq. (S20). This numerical computation yields the plots in Figs. 4 and 5 of the main manuscript.

We use discretized variables  $X_m \equiv X(\rho = m/N)$ , with integer  $m \in [0, N]$ . Equation (S20) then becomes

$$-\frac{1}{N} = R_m Z_m - L_m Z_{m-1}, \quad (\text{S23})$$

where  $Z_m \equiv T_{m+1} - T_m$ . With the boundary conditions  $T_m = T_{N-m}$  and  $T_0 = T_N = 0$ , we obtain  $Z_{\frac{N}{2}-1} = \frac{1}{2NR_{\frac{N}{2}}}$  and  $Z_0 = T_1$ . We use Eq. (S23) to determine  $Z_m$  for the other values of  $m$ . We obtain  $T_m$  by calculating

$$T_m = \sum_{l=0}^{m-1} Z_l. \quad (\text{S24})$$

## 2. Derivation of the logarithmic scalings of $T(\rho)$ and $\tau$

The numerical computation of  $T(\rho)$  in Sec. S2C 1 is useful, but it does not provide sufficient intuition about  $T(\rho)$ . To obtain such intuition, we perform an approximate analytical calculation by neglecting the second-order (i.e., diffusion) term in Eq. (S22). The rationale behind neglecting the diffusion term is that  $D(\rho)$ , which includes the factor  $1/N$ , is much smaller than the drift term  $v(\rho)$ . We thus expect to extract the correct leading-order scaling for  $T(\rho)$  under this approximation. With the boundary conditions  $T(\rho = 0) = T(\rho = 1) = 0$ , the solution of the approximate Eq. (S22) satisfies

$$T(\rho) \approx \int_{\frac{1}{N}}^{\rho} \frac{-1}{v(\rho')} d\rho', \quad (\text{S25})$$

where we set the lower limit of the integral to  $1/N$  to keep track of the  $N$ -dependence of  $T(\rho)$ . The drift function  $v(\rho)$  is given by Eq. (S13). For an  $s$ -uniform hypergraph, Eq. (S13) is

$$v(\rho) = \frac{\rho(1-\rho)}{(s-1)^{q-1}} \sum_{r=1}^{q-1} A_{r,q} [\rho^r - (1-\rho)^r] \prod_{l=1}^r (s-1-l). \quad (\text{S26})$$

The factor  $\rho^r - (1-\rho)^r$  in Eqs. (S13,S26) becomes 0 only when  $\rho = 1/2$  because the function  $\rho^r$  is a bijection. Furthermore,

$$\left. \frac{\rho^r - (1-\rho)^r}{(2\rho-1)} \right|_{\rho=\frac{1}{2}} = r \left( \frac{1}{2} \right)^{r-1},$$

so  $\rho = 1/2$  is a simple root. We thus write the drift function  $v(\rho)$  as

$$v(\rho) = \rho(1-\rho)(2\rho-1)f(\rho, s, q), \quad (\text{S27})$$

where  $f(\rho, s, q)$  does not contain real zeroes of  $\rho$ . Performing a partial-fraction expansion of Eq. (S27) yields

$$\frac{1}{v(\rho)} = \frac{C_1(s, q)}{\rho} + \frac{C_2(s, q)}{(1-\rho)} + \frac{C_3(s, q)}{(2\rho-1)} + \frac{g(\rho, s, q)}{f(\rho, s, q)}, \quad (\text{S28})$$

which we insert into Eq. (S25) to obtain the approximate exit time.

We first compute the exit time  $\tau \equiv T(\rho = 1/2)$  from the balanced initial condition (with the same number of nodes in each state). We obtain

$$\tau(s, q, N) \equiv T(\rho = 1/2) \approx \int_{\frac{1}{2} - \frac{1}{\sqrt{N}}}^{\frac{1}{2}} \frac{1}{v(\rho')} d\rho' \sim \left( -C_1 + \frac{C_3}{4} \right) \ln N \equiv \mathcal{A}(s, q) \ln N, \quad (\text{S29})$$

where we offset the initial density by  $1/\sqrt{N}$  from  $1/2$  both to avoid getting trapped in the equilibrium point  $\rho = 1/2$  and to account for intrinsic stochasticity. The notation  $\sim$  signifies the leading-order scaling in  $N$ . The expression for  $C_1(s, q)$  is

$$C_1(s, q) \equiv \left. \frac{\rho}{v(\rho)} \right|_{\rho=0} = \frac{(s-1)^{q-1}}{-\sum_{r=1}^{q-1} A_{r,q} \prod_{l=1}^r (s-1-l)} = \frac{(s-1)^{q-1}}{1 - (s-1)^{q-1}}, \quad (\text{S30})$$

where the last equality follows from  $\sum_{r=1}^{q-1} A_{r,q} \prod_{l=1}^r (s-1-l) = \left. \frac{(s-1)^{q-1} R(\rho)}{\rho(1-\rho)} \right|_{\rho=1} - 1 = (s-1)^{q-1} - 1$  by using Eq. (S3).

The expression for  $C_3(s, q)$  is

$$C_3(s, q) \equiv \left. \frac{(2\rho-1)}{v(\rho)} \right|_{\rho=\frac{1}{2}} = \frac{4(s-1)^{q-1}}{\sum_{r=1}^{q-1} r \left( \frac{1}{2} \right)^{r-1} A_{r,q} \prod_{l=1}^r (s-1-l)}. \quad (\text{S31})$$

Therefore, the leading-order behavior of  $\tau(s, q, N)$  as  $N \rightarrow \infty$  is

$$\tau(s, q, N) \sim \left[ \frac{(s-1)^{q-1}}{(s-1)^{q-1} - 1} + \frac{(s-1)^{q-1}}{\sum_{r=1}^{q-1} r \left( \frac{1}{2} \right)^{r-1} A_{r,q} \prod_{l=1}^r (s-1-l)} \right] \ln N, \quad (\text{S32})$$

which is one of the main theoretical results of our paper. It shows the logarithmic scaling of  $\tau$  with  $N$  for the generic GVM for  $q \geq 2$  and  $s \geq 3$ .

### 3. Explicit derivation of the formulas for $\tau$ in the main manuscript

We now obtain the explicit leading-order formulas for  $\tau$  in the main manuscript from the general formula Eq. (S32). When  $q = 2$ , Eq. (S32) becomes

$$\begin{aligned}\tau(s, q = 2, N) &\sim \left[ \frac{(s-1)}{(s-2)} + \frac{(s-1)}{A_{1,2}(s-2)} \right] \ln N \\ &= \frac{2(s-1)}{(s-2)} \ln N,\end{aligned}\tag{S33}$$

which is Eq. (8) of the main manuscript. When  $q = 5$ , Eq. (S32) becomes

$$\begin{aligned}\tau(s, q = 5, N) &\sim \left[ \frac{(s-1)^4}{(s-1)^4 - 1} + \frac{(s-1)^4}{\sum_{r=1}^4 r \left(\frac{1}{2}\right)^{r-1} A_{r,5} \prod_{l=1}^r (s-1-l)} \right] \ln N \\ &= \left\{ \frac{(s-1)^4}{(s-1)^4 - 1} + \frac{(s-1)^4}{(s-2) [A_{1,5} + (s-3)A_{2,5} + \frac{3}{4}(s-3)(s-4)A_{3,5} + \frac{1}{2}(s-3)(s-4)(s-5)A_{4,5}]} \right\} \ln N \\ &= \frac{(s-1)^4(3s-4)(s+1)}{s(s-2)(s^2+3s-8)(s^2-2s+2)} \ln N,\end{aligned}\tag{S34}$$

which is Eq. (9) of the main manuscript. The exit time  $\tau$  diverges for  $s = 2$  in Eq. (S32), so it also diverges in Eqs. (S33) and (S34).

For  $s = N$  with  $N \gg 1$ , the denominator of  $C_3$  is dominated by the order- $(q-1)$  term

$$\sum_{r=1}^{q-1} r \left(\frac{1}{2}\right)^{r-1} A_{r,q} \prod_{l=1}^r (s-1-l) \approx \frac{(q-1)}{2^{q-2}} (s-1)^{q-1}.$$

Therefore, for  $s = N$ , Eq. (S32) becomes

$$\tau(q, N) \sim \left[ 1 + \frac{2^{q-2}}{(q-1)} \right] \ln N,\tag{S35}$$

which is Eq. (10) of the main manuscript. Equation (S35) also applies to the  $q$ -voter model on complete (i.e., fully-connected) dyadic networks, and it agrees with the results for  $q = 2$  and  $q = 3$  in Ref. [S2].

When  $s$  is finite, it is convenient to replace the upper limit  $r = q-1$  of the sum  $\sum_{r=1}^{q-1} r \left(\frac{1}{2}\right)^{r-1} A_{r,q} \prod_{l=1}^r (s-1-l)$  by  $r = s-2$ . For example, when we do this, Eq. (S32) becomes

$$\begin{aligned}\tau(s = 3, q, N) &\approx \left( \frac{2^{q-1}}{2^{q-1} - 1} + \frac{2^{q-1}}{A_{1,q}} \right) \ln N \\ &= \left( \frac{2^q}{2^{q-1} - 1} \right) \ln N,\end{aligned}\tag{S36}$$

$$\begin{aligned}\tau(s = 5, q, N) &\approx \left[ \frac{4^{q-1}}{4^{q-1} - 1} + \frac{4^{q-1}}{\sum_{r=1}^3 r \left(\frac{1}{2}\right)^{r-1} A_{r,q} \prod_{l=1}^r (4-l)} \right] \ln N \\ &= \left[ \frac{4^{q-1}}{4^{q-1} - 1} + \frac{4^q}{3(4^{q-1} + 3^{q-1} - 2^{q-1} - 1)} \right] \ln N \\ &= \frac{4^{q-1}}{4^{q-1} - 1} \left[ \frac{\frac{7}{3}(4^{q-1} - 1) + 3^{q-1} - 2^{q-1}}{4^{q-1} - 1 + 3^{q-1} - 2^{q-1}} \right] \ln N\end{aligned}\tag{S37}$$

for  $s = 3$  and  $s = 5$ .

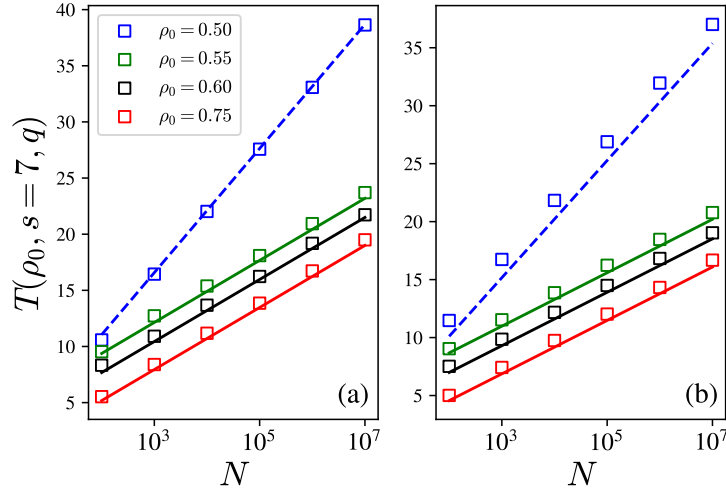


FIG. S2. The exit time  $T(\rho_0)$  of the GVM on annealed 7-uniform hypergraphs for different initial densities  $\rho_0$  when (a)  $q = 2$  and (b)  $q = 5$ . The symbols give the means of  $10^6$  (when  $N \leq 10^4$ ) or  $10^3$  (when  $N \geq 10^5$ ) independent MC simulations on  $N$ -node hypergraphs. The solid lines correspond indicate theoretical results from Eq. (S39) and Eq. (S41). We obtain the dashed lines from Eqs. (S33) and (S34).

#### 4. Dependence of the exit time $T(\rho_0)$ on the initial density $\rho_0$

We now compute the initial density-dependent exit time  $T(\rho_0)$  under the approximation of Eq. (S25). From Eqs. (S25) and (S28), the leading-order expression for  $T(\rho_0)$  for the initial density  $\rho_0$  away from  $\rho_0 = 1/2$  takes the form  $T(\rho_0) \approx -C_1 \ln N + T_0(\rho_0)$ . That is, it scales as  $\ln N$  with a  $\rho_0$ -independent amplitude  $-C_1$  and  $\rho_0$ -dependent integration constant  $T_0(\rho_0)$ .

We elaborate on the derivation of  $T(\rho_0)$  for some values of  $q$ . The approximate backward Kolmogorov equations for both  $q = 2$  and  $q = 3$  have the form

$$v(\rho) = \frac{(s-1)^{q-1} - 1}{(s-1)^{q-1}} \rho(1-\rho)(2\rho-1), \quad (\text{S38})$$

from which we obtain

$$\begin{aligned} T(\rho_0, s, q) &\approx \int_{\rho_0}^{\frac{1}{N}} \frac{(s-1)^{q-1}}{[(s-1)^{q-1} - 1] \rho'(1-\rho')(2\rho'-1)} d\rho' \\ &= \frac{(s-1)^{q-1}}{[(s-1)^{q-1} - 1]} \ln \left[ \frac{(1 - \frac{2}{N})^2 \rho_0(1-\rho_0)}{(1-2\rho_0)^2 \frac{1}{N}(1-\frac{1}{N})} \right] \\ &\approx \frac{(s-1)^{q-1}}{[(s-1)^{q-1} - 1]} \ln \left[ \frac{N\rho_0(1-\rho_0)}{(1-2\rho_0)^2} \right], \end{aligned} \quad (\text{S39})$$

where the last step uses the fact that  $N \gg 1$ . Equation (S39) with  $s \rightarrow \infty$  is equivalent to Eq. (17) of Ref. [S2].

For  $q = 4$  and  $q = 5$ , the drift function is

$$v(\rho) = \rho(1-\rho)(2\rho-1) [a(s, q)\rho^2 - a(s, q)\rho + b(s, q)], \quad (\text{S40})$$

where  $a(s, q = 4) = \frac{(s-2)(s-3)(s-4)}{(s-1)^3}$ ,  $a(s, q = 5) = \frac{2s(s-2)(s-3)(s-4)}{(s-1)^4}$ , and  $b(s, q) = \frac{(s-1)^{q-1} - 1}{(s-1)^{q-1}}$ . The exit time  $T(\rho_0 > 1/2)$



is

$$\begin{aligned}
T(\rho_0, s, q) &\approx \int_{1-\rho_0}^{\frac{1}{N}} \frac{d\rho'}{\rho'(1-\rho')(2\rho'-1)[a(s, q)\rho'^2 - a(s, q)\rho' + b(s, q)]} \\
&= \int_{1-\rho_0}^{\frac{1}{N}} \frac{1}{b(s, q)} \left[ \frac{1}{(1-\rho')} - \frac{1}{\rho'} \right] + \frac{4}{\left[ b(s, q) - \frac{a(s, q)}{4} \right] (2\rho' - 1)} + \left[ \frac{1}{b(s, q) \left[ 1 - \frac{4b(s, q)}{a(s, q)} \right]} \right] \frac{2\rho' - 1}{\rho'^2 - \rho' + \frac{b(s, q)}{a(s, q)}} d\rho' \\
&= \frac{1}{b(s, q)} \ln \left[ \frac{(1-\rho_0)\rho_0}{\left(1 - \frac{1}{N}\right) \frac{1}{N}} \right] + \frac{2}{\left[ b(s, q) - \frac{a(s, q)}{4} \right]} \ln \left( \frac{1 - \frac{2}{N}}{2\rho_0 - 1} \right) + \frac{1}{b(s, q) \left[ 1 - \frac{4b(s, q)}{a(s, q)} \right]} \ln \left[ \frac{\frac{1}{N^2} - \frac{1}{N} + \frac{b(s, q)}{a(s, q)}}{\rho_0^2 - \rho_0 + \frac{b(s, q)}{a(s, q)}} \right] \\
&\approx \frac{1}{b(s, q)} \ln[N\rho_0(1-\rho_0)] - \frac{2}{\left[ b(s, q) - \frac{a(s, q)}{4} \right]} \ln(2\rho_0 - 1) + \frac{1}{b(s, q) \left[ 1 - \frac{4b(s, q)}{a(s, q)} \right]} \ln \left[ \frac{\frac{b(s, q)}{a(s, q)}}{\rho_0^2 - \rho_0 + \frac{b(s, q)}{a(s, q)}} \right] \quad (\text{S41})
\end{aligned}$$

when  $N \gg 1$ . We confirm Eqs. (S39) and (S41) using MC simulations (see Fig. S2).

### S3. VARIANTS OF OUR GVM

#### A. Simplicial GVM

In the simplicial GVM, a node flips its opinion in stage (iii) if the opinions of all of its  $s-1$  neighbors' opinions are different from its opinion. Therefore, the raising and the lowering operators are

$$\begin{aligned}
R(\rho) &= \frac{\sum_s sP(s)(1-\rho)\rho^{s-1}}{\sum_s sP(s)}, \\
L(\rho) &= \frac{\sum_s sP(s)\rho(1-\rho)^{s-1}}{\sum_s sP(s)}. \quad (\text{S42})
\end{aligned}$$

We can insert the transition probabilities  $R(\rho)$  and  $L(\rho)$  into Eq. (S20) to obtain a recursion relation for the exit time  $T(\rho)$ .

To obtain a leading-order approximation of  $\tau$ , we write the drift function  $v(\rho)$  as

$$v(\rho) = \frac{\rho(1-\rho)}{\sum_s sP(s)} \sum_s sP(s) [\rho^{s-2} - (1-\rho)^{s-2}], \quad (\text{S43})$$

from which we obtain

$$\begin{aligned}
\tau &\sim \left[ -\frac{\rho}{v(\rho)} \Big|_{\rho=0} + \frac{2\rho-1}{4v(\rho)} \Big|_{\rho=\frac{1}{2}} \right] \ln N \\
&= \left[ \frac{1}{1 - \frac{2P(2)}{\langle s \rangle}} + \frac{\langle s \rangle}{\sum_{s=3}^N s(s-2) \left( \frac{1}{2} \right)^{s-3} P(s)} \right] \ln N. \quad (\text{S44})
\end{aligned}$$

We again obtain a  $\ln N$  scaling with system size. For instance, for an  $s$ -uniform hypergraph with  $s \geq 3$ , we obtain

$$\tau \sim \left[ 1 + \frac{2^{s-3}}{(s-2)} \right] \ln N, \quad (\text{S45})$$

which is equivalent to Eq. (S35) for  $q = s-1$ .

In Fig. 2 of the main manuscript, we showed the results of MC simulations of the simplicial GVM on annealed hypergraphs with two different hyperedge-size distributions  $P(s)$ . We now compare these simulation results with analytical results.

First, we consider the geometric hyperedge-size distribution  $P(s) = \frac{1}{\mu-1} \left( \frac{\mu-2}{\mu-1} \right)^{s-2}$  for  $s \geq 2$  with mean hyperedge size  $\mu$ . For this distribution, Eq. (S44) becomes

$$\tau \sim \left( \frac{\mu}{\mu-2} \right) \left[ \frac{\mu-1}{\mu+1} + \frac{\mu^3}{4(5\mu-4)} \right] \ln N, \quad (\text{S46})$$

which predicts that  $\tau$  exhibits optimality with a minimum value at  $\mu^* \approx 3.58$ .

We now consider the power-law hyperedge-size distribution with the exponent  $\alpha$ . This distribution has the formula  $P(s) = \frac{s^{-\alpha}}{\zeta(\alpha)-1}$  for  $s \geq 2$  and the mean hyperedge size  $\frac{\zeta(\alpha-1)-1}{\zeta(\alpha)-1}$ , where  $\zeta(z)$  is the Riemann zeta function. For this distribution, Eq. (S44) becomes

$$\begin{aligned} \tau &\sim \left( \sum_{s=2}^N s^{1-\alpha} \right) \left[ \frac{1}{\sum_{s=3}^N s^{1-\alpha}} + \frac{1}{\sum_{s=3}^N \frac{(s-2)s^{1-\alpha}}{2^{s-3}}} \right] \ln N \\ &\approx [\zeta(\alpha-1) - 1] \left[ \frac{1}{\zeta(\alpha-1) - 1 - 2^{1-\alpha}} + \frac{1}{8\text{Li}_{\alpha-2}\left(\frac{1}{2}\right) - 16\text{Li}_{\alpha-1}\left(\frac{1}{2}\right) + 4} \right] \ln N, \end{aligned} \quad (\text{S47})$$

where  $\text{Li}_s(z)$  is the polylogarithm function and the last step follows by taking the upper limit of the sums to  $\infty$ . Equation (S47) predicts that  $\tau$  exhibits optimality with a minimum value at  $\alpha^* \approx 2.87$ .

As we showed in Fig. 2 of the main manuscript, the theory agrees well with the results of MC simulations. The numerical solution of the recursion relation (S20) (solid curves) agrees very well with the results of MC simulations; the leading-order approximations (S46,S47) (dotted curve) successfully account for the optimality and the existence of minimum  $\tau$ .

The expression (S44) for  $\tau$  for the simplicial GVM diverges when  $\langle s \rangle \downarrow 2$  because it approaches the situation for a dyadic network and  $\tau$  crosses over to the diffusive behavior  $\mathcal{O}(N)$  in this limit. This situation corresponds to the  $\mu \downarrow 2$  limit of Eq. (S46) and the  $\alpha \rightarrow \infty$  limit of Eq. (S47), respectively.

### B. GVM without duplicate selections

Our analysis also applies if we disallow duplicate selections in the neighbor-selection stage (iii) of the GVM (see Sec. S1 B). In this case, the raising operator  $R(\rho)$  and lowering operator  $L(\rho)$  are

$$\begin{aligned} R(\rho) &= \frac{(1-\rho)}{\sum_s sP(s)} \sum_s sP(s) \sum_{n=q}^{s-1} \frac{(s-1)!}{n!(s-1-n)!} \rho^n (1-\rho)^{s-1-n} \frac{\frac{n!}{q!(n-q)!}}{\frac{(s-1)!}{q!(s-1-q)!}} \\ &= \frac{(1-\rho)}{\sum_s sP(s)} \sum_s sP(s) \sum_{n=q}^{s-1} \frac{(s-1-q)!}{(n-q)!(s-1-n)!} \rho^n (1-\rho)^{s-1-n} \\ &= \frac{(1-\rho)}{\sum_s sP(s)} \sum_s sP(s) \rho^q, \end{aligned} \quad (\text{S48})$$

$$L(\rho) = \frac{\rho}{\sum_s sP(s)} \sum_s sP(s) (1-\rho)^q. \quad (\text{S49})$$

When  $s = N$ , these formulas are equivalent to those for the GVM with duplicate selections allowed. Therefore, for  $s = N$ , we obtain the same formula for the exit time. On an annealed  $s$ -uniform hypergraph,

$$\tau(q, N) \sim \left[ 1 + \frac{2^{q-2}}{(q-1)} \right] \ln N, \quad (\text{S50})$$

which is valid for  $q \leq s-1$ . In Fig. S3, we show results for  $q = 2$  with  $\tau \sim 2 \ln N$ .

### C. GVM with edge-update dynamics

Similar to Glauber versus Kawasaki dynamics in the kinetic Ising model [S3], one can frame standard VM dynamics in terms of edge-update rules, rather than the node-update rules (which we discussed in the main manuscript). In each step of an MC simulation, we (i) choose an edge uniformly at random and (ii) update the states of both of its attached edges to the same uniformly-randomly-chosen state when they have different states [S4]. An equivalent way to implement (ii) is to select a uniformly random node that is attached to the edge and copy its state to the other node. We now generalize such edge-update dynamics to hypergraphs using the hyperedge-wise collective state flippings.

We consider the following GVM with edge-update dynamics. At each time step, an MC simulation has the following stages:

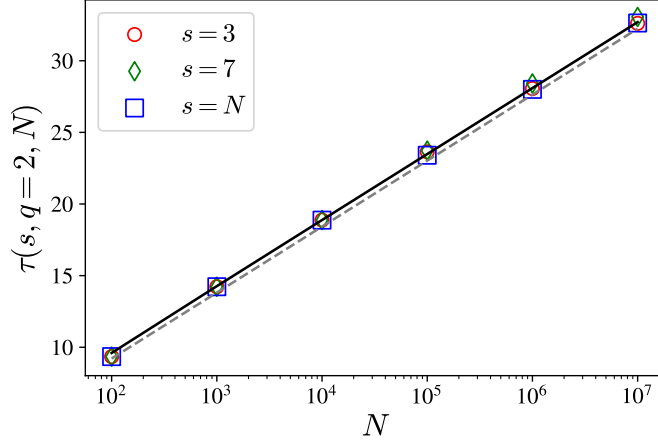


FIG. S3. Dependence of the exit time  $\tau$  on the system size  $N$  for a GVM without duplicate selections for nonlinearity strength  $q = 2$  and hyperedge sizes  $s = 3$ ,  $s = 7$ , and  $s = N$ . The markers indicate the means of  $10^6$  (when  $N \leq 10^4$ ) or  $10^3$  (when  $N \geq 10^5$ ) independent MC simulations on annealed  $s$ -uniform hypergraphs. The lines indicate solutions from the recursion relation (S20) (solid) and the leading-order solution (S50) (dotted).

(i) We select a size- $s$  hyperedge  $h$  uniformly at random.

(ii-a) We select  $q$  distinct nodes uniformly at random from the  $s$  nodes that are attached to  $h$ .

(ii-b) If all of the  $q$  nodes that we select in (ii-a) have the same state, then we copy this state to every node that is attached to  $h$ .

In stage (ii-b), the nodes with a state that is different from the  $q$  nodes flip their state. In general, a time step can include more than one such node, which is a crucial distinction from the node-update GVM in the main manuscript. Additionally, in (ii-a), we disallow duplicate selections of nodes. This is for technical convenience; one obtains qualitatively similar results if one allows duplicates.

From the model definition, we can readily write the transition probabilities for our edge-update GVM. The raising operator  $R_{s,n}(\rho) \equiv P(\rho \rightarrow \rho + \delta\rho_{s,n}^+)$ , with  $\delta\rho_{s,n}^+ \equiv (s-n)/N$ , is the transition probability that a hypergraph has  $s-n$  more nodes in state **1** after the a time step. It is given by

$$\begin{aligned} R_{s,n}(\rho) &= P(s) \frac{s!}{n!(s-n)!} \rho^n (1-\rho)^{s-n} \frac{\frac{n!}{q!(n-q)!}}{s!} \\ &= P(s) \frac{(s-q)!}{(s-n)!(n-q)!} \rho^n (1-\rho)^{s-n}. \end{aligned} \quad (\text{S51})$$

The lowering operator  $L_{s,n}(\rho) \equiv P(\rho \rightarrow \rho - \delta\rho_{s,n}^-)$ , with  $\delta\rho_{s,n}^- \equiv n/N$ , the transition probability that a hypergraph has  $n$  more nodes in state **0** after a time step. It is given by

$$\begin{aligned} L_{s,n}(\rho) &= P(s) \frac{s!}{n!(s-n)!} \rho^n (1-\rho)^{s-n} \frac{\frac{(s-n)!}{q!(s-n-q)!}}{s!} \\ &= P(s) \frac{(s-q)!}{(s-n-q)!n!} \rho^n (1-\rho)^{s-n}. \end{aligned} \quad (\text{S52})$$

The recursion relation for the exit time  $T(\rho)$  is

$$T(\rho) = \sum_{s,n} [R_{s,n}(\rho)T(\rho + \delta\rho_{s,n}^+) + L_{s,n}(\rho)T(\rho - \delta\rho_{s,n}^-)] + \left[ 1 - \sum_{s,n} R_{s,n}(\rho) + L_{s,n}(\rho) \right] T(\rho) + \delta t, \quad (\text{S53})$$

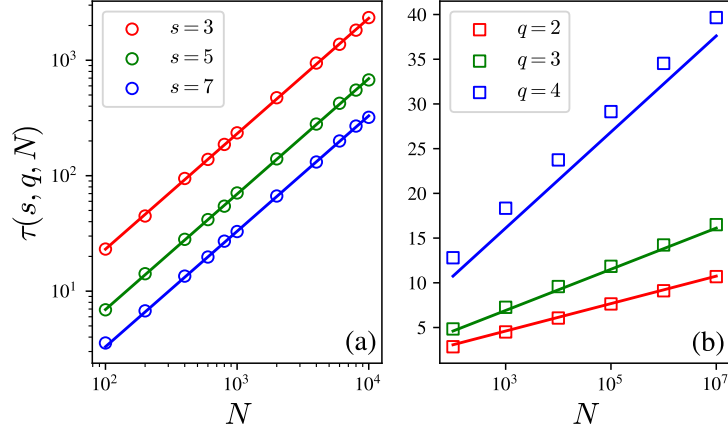


FIG. S4. Dependence of  $\tau(s, q, N)$  on the hypergraph size  $N$ . The markers indicate means of  $10^3$  independent MC simulations on annealed  $s$ -uniform hypergraphs. (a) A nonlinearity strength of  $q = 1$ . The lines are solutions of  $\tau(s, q = 1, N) = \frac{2N \ln 2}{s(s-1)}$  from Eq. (S58) for different values of  $s$ . (b) Nonlinearity strengths of  $q \geq 2$ . We obtain the lines from Eq. (S59) for different values of  $q$  for  $s = 5$ .

which yields the backward Kolmogorov equation

$$\begin{aligned}
 -1 &= \left[ \sum_s P(s)(s-q) \{ (1-\rho)\rho^q - \rho(1-\rho)^q \} \right] \frac{\partial T(\rho)}{\partial \rho} \\
 &+ \left[ \sum_s P(s) \frac{(s-q)}{2N} \{ (s-q-1)\rho^q(1-\rho)^2 + \rho^q(1-\rho) + (s-q-1)(1-\rho)^q\rho^2 + (1-\rho)^q\rho \} \right] \frac{\partial^2 T(\rho)}{\partial \rho^2} \\
 &\equiv v_h(\rho) \frac{\partial T(\rho)}{\partial \rho} + D_h(\rho) \frac{\partial^2 T(\rho)}{\partial \rho^2}.
 \end{aligned} \tag{S54}$$

In our derivation of Eq. (S54) from Eq. (S53), we use the Taylor expansion of  $T(\rho \pm \delta\rho_{s,n}^\pm)$  in  $\delta\rho_{s,n}^\pm$  to second order:

$$T(\rho \pm \delta\rho_{s,n}^\pm) \approx T(\rho) \pm \frac{\partial T(\rho)}{\partial \rho_{s,n}^\pm} \delta\rho_{s,n}^\pm + \frac{1}{2} \frac{\partial^2 T(\rho)}{\partial \rho^2} (\delta\rho_{s,n}^\pm)^2. \tag{S55}$$

When  $q = 1$ , the drift function  $v_h(\rho) = 0$ , so Eq. (S54) reduces to

$$-1 = \frac{(\langle s^2 \rangle - \langle s \rangle)\rho(1-\rho)}{2N} \frac{\partial^2 T(\rho)}{\partial \rho^2}, \tag{S56}$$

where  $\langle s^r \rangle \equiv \sum_s s^r P(s)$ . The solution of Eq. (S56) is

$$T(\rho) = \frac{2N}{(\langle s^2 \rangle - \langle s \rangle)} \left[ \rho \ln \frac{1}{\rho} + (1-\rho) \ln \left( \frac{1}{1-\rho} \right) \right]. \tag{S57}$$

The exit time  $\tau$  is

$$\tau(q=1) \equiv T(\rho=1/2) = \frac{2 \ln 2}{\langle s^2 \rangle - \langle s \rangle} N \propto N. \tag{S58}$$

In Fig. S4(a), we confirm Eq. (S58) when  $q = 1$ . When  $s = 2$ , Eq. (S58) reduces to the exit time for VM dynamics in dyadic networks.

When  $q \geq 2$ , Eq. (S54) is not analytically solvable. Therefore, we apply the same approximation procedure as in Sec. S2 C and obtain an approximate solution of  $\tau$  by substituting  $v_h(\rho)$  into Eq. (S29) and keeping the leading-order (in  $N$ ) terms. The exit time  $\tau$  is then

$$\tau(q \geq 2) \sim \frac{1}{\sum_{s \geq q+1} P(s)(s-q)} \left[ 1 + \frac{2^{q-2}}{(q-1)} \right] \ln N, \tag{S59}$$

which again scales logarithmically in  $N$ . In Fig. S4(b), we compare this analytical prediction with the results of MC simulations on annealed  $s$ -uniform hypergraphs. We obtain reasonable agreement.

---

[S1] V. Sood and S. Redner, Phys. Rev. Lett. **94**, 178701 (2005).

[S2] L. S. Ramirez, F. Vazquez, M. San Miguel, and T. Galla, Phys. Rev. E **109**, 034307 (2024).

[S3] P. L. Krapivsky, S. Redner, and E. Ben-Naim, *A Kinetic View of Statistical Physics* (Cambridge University Press, Cambridge, UK, 2010).

[S4] K. Suchecki, V. M. Eguíluz, and M. San Miguel, Europhys. Lett. **69**, 228 (2005).